Frustration and magnetism of the zigzag chain compounds EuL_2O_4 (L = Yb, Lu, Gd, Eu)

Oren Ofer,[1,*] Jun Sugiyama,[2] Jess H. Brewer,[3] Eduardo J. Ansaldo,[4] Martin Månsson,[5,6] Kim H. Chow,[7] Kazuya Kamazawa,[2,†] Yoshihiro Doi,[8] and Yukio Hinatsu[8]

[1]*TRIUMF, 4004 Wesbrook Mall, Vancouver, British Columbia, Canada V6T 2A3*

[2]*Toyota Central Research and Development Laboratories Inc., Nagakute, Aichi 480-1192, Japan*

[3]*Department of Physics and Astronomy, University of British Columbia, Vancouver, British Columbia, Canada V6T 1Z1*

[4]*Department of Physics, University of Saskatchewan, Saskatoon, Saskatchewan, Canada S7N 0W0*

[5]*Laboratory for Neutron Scattering, ETH Zürich and Paul Scherrer Institute, CH-5232 Villigen PSI, Switzerland*

[6]*Laboratory for Solid State Physics, ETH Zürich, CH-8093 Zürich, Switzerland*

[7]*Department of Physics, University of Alberta, Edmonton, Alberta, Canada T6G 2G7*

[8]*Division of Chemistry, Hokkaido University, Sapporo, Hokkaido 060-0810, Japan*

(Received 15 June 2011; published 9 August 2011)

We present muon-spin rotation/relaxation and susceptibility measurements on polycrystalline samples of EuL_2O_4, where L is the lanthanide Yb, Lu, Gd, or Eu. The magnetic phase of these quasi-one-dimensional *zigzag* chain compounds is characterized with respect to the difference in their lanthanide magnetic moment. We find that the magnetic phase varies systematically with the lanthanide magnetic moment. At zero lanthanide moments ($EuLu_2O_4$), we find a static antiferromagnetic phase; as the moment increases, the phase gradually changes to an incommensurate spin-density-wave ordered phase, and finally reaches a dynamic phase, when large lanthanide magnetic moments are present ($EuGd_2O_4$).

DOI: 10.1103/PhysRevB.84.054428 PACS number(s): 75.25.−j, 75.30.Cr, 75.50.Ee, 76.75.+i

I. INTRODUCTION

One-dimensional systems that contain competing nearest-neighbor (NN) and next-nearest-neighbor (NNN) interactions offer an intriguing example of relatively simple systems which show fascinating magnetic phenomena and complex multiple phases. Over the last decade, the successful synthesis of one-dimensional (1D) *zigzag* chains has presented a remarkable diversity of magnetic phenomena, inspiring experimental[1–5] and theoretical[6,7] studies. Such theoretical studies have shown that the XXZ Hamiltonian, appropriate for quasi-1D systems, can be characterized by only two parameters. Interestingly, this model is shown to contain multiple phases: e.g., vector chiral orders, dimer orders, Néel order, and a Tomonaga-Luttinger liquid.[8] This scenario has also been shown in the presence of an external field in the Heisenberg model.[9,10] Thus, the question arises whether we can control the magnitude of the magnetic moments of the *zigzag* chain and use it as a tuning parameter to manipulate the magnetic frustration-ground state interplay in these systems. Here we attempt to answer this question by studying new compounds, in which the frustration is tuned by the chemical substitution of the magnetic ions.

The EuL_2O_4 compounds, where L is a lanthanide element, are composed of a L *zigzag* chains with a honeycomb-like structure formed by these chains, with the crystallographic $CaFe_2O_4$ (CFO)-type $Pnma$ structure.[11] The schematic structure is shown in the inset of Fig. 1 where possible exchange paths which create an $\hat{a}\hat{c}$-plane honeycomb lattice as well the *zigzag* along the $\hat{b}$ axis are suggested by the black lines. This crystallographic structure is the basis of numerous recently reported quasi-1D *zigzag* chains.[12,13] Due to the high neutron absorption cross section by Eu, neutron scattering experiments on such compounds are challenging; thus, μSR has a key advantage in this case for providing information on the magnetic interactions. Here, we report on an extensive μSR study of EuL_2O_4, where L = Eu, Gd, Yb, and Lu, in order to clarify their magnetic nature with respect to their frustration. The lanthanides Eu, Gd, Yb, and Lu are very similar in their atomic and electronic properties. Consequently, comparative studies on EuL_2O_4 allow a unique comparison of the magnetic interactions, since Yb, Gd, and Eu have different magnetic moments, while Lu has none. Hence, we are able to probe how the magnetic ground state is affected, from a situation where there are no magnetic *zigzag* chains, or no frustration along the *zigzag* ladders when there is no magnetic moment (in L = Lu), to a state where we have intense frustration with a large magnetic moment (as in L = Gd). Naturally, the increase in the magnetic moment can influence the ground state by embodying high-order perturbation such as NNN interactions, hence this study could potentially provide theorists an interesting challenge: to predict high-order perturbations and the resulting ground state due to the increase of the magnetic moment in this system.

Similar compounds, SrL_2O_4 (Ref. 14) and BaL_2O_4,[15] were reported to show an anomaly in susceptibility measurements, which is ascribed to the magnetic interaction between the L^{3+} ions. This is because the alkali ions, Sr^{2+} and Ba^{2+}, should not contribute to the magnetism due to their diamagnetic nature. By contrast, the Eu^{2+} ions at the alkali site in EuL_2O_4 are expected to introduce additional magnetic interactions with the L^{3+} ions, thus affecting the magnetic behavior, due to their large magnetic moment and partially occupied $4f$ orbital.

The manuscript is organized as follows: in Sec. II, we illustrate the EuL_2O_4 experimental details on the preparation and the magnetic characterization using bulk magnetization and μSR. In Sec. III, we present the results from the μSR measurements and describe the analysis following by a discussion.

II. EXPERIMENT

Polycrystalline EuL_2O_4 samples were prepared at Hokkaido University by a solid-state reaction between EuO

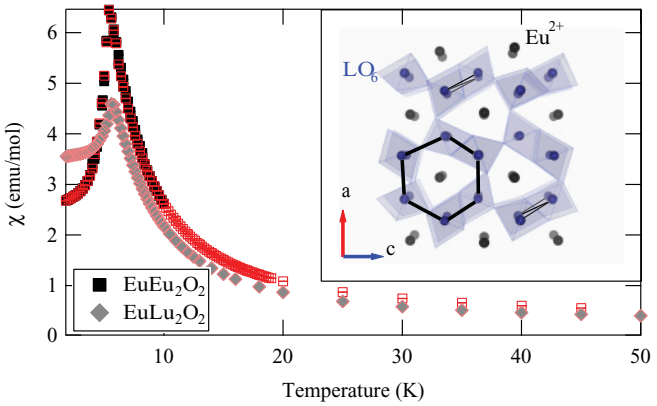

FIG. 1. (Color online) Temperature dependence of the zero-field-cooled (hollow symbols) and field-cooled (filled symbols) susceptibilities of $EuEu_2O_4$ and $EuLu_2O_4$. (Inset) The $CaFe_2O_4$-type crystal structure (space group $Pnma$, no. 62) of EuL_2O_4. Dark (black) and light (blue) spheres represent the Eu^{2+} and L^{3+} ions, respectively. Solid black lines indicate the $\hat{a}\hat{c}$-plane honeycomb (thick) and $\hat{b}$ axis triangular lattice (thin) incorporating the *zigzag* chains.

and L_2O_3 in an evacuated quartz tube at 1373 K for 24 h, as described in Ref. 11. Prior to this reaction, EuO was prepared by heating mixtures of Eu metal and Eu_2O_3 in a quartz tube at 1073 K for 24 h. dc-χ measurements and powder diffraction (Cu$K\alpha$ radiation) analyses for the present samples yielded reproducible results consistent with those in a previous report.[11]

Bulk susceptibility (χ) of EuL_2O_4 were measured using a Quantum Design Magnetic Properties Measurement System superconducting quantum interference device (SQUID). These χ measurements showed that these EuL_2O_4 compounds are very similar in their bulk magnetic behavior showing an antiferromagnetic (AF) transition at $T \approx 6$ K (for example, SQUID magnetometer measurements of $L =$ Eu, Lu are presented in Fig. 1, and for $L =$ Gd and Yb are shown in Figs. 4 and 5, respectively). Hence the 3D nature of the transition is mainly controlled by the Eu^{2+} ion. Although bulk χ measurements on $EuLu_2O_4$ indicate the formation of AF order below $T_N = 5.7$ K, its positive Curie-Weiss temperature [$\Theta_{CW} = 9.8(7)$ K] suggests a predominance ferromagnetic (FM) interaction of the magnetic Eu^{+2} ions. The suggested resolution is a FM coupling between NN Eu^{2+} ions together with AF interaction between parallel Eu^{2+} 1D chains, realizing an overall AF structure.[11] Note that the Lu^{3+} ion's $4f$ orbitals are fully occupied, resulting in the nonmagnetic nature of the Lu^{3+} ions. A Curie law fitting of χ at $200 \leqslant T \leqslant 400$ K reveals the effective magnetic moment to be $\mu_{\text{eff}} = 7.94(2)\mu_B$ as expected from the Eu^{2+} ions. This enables us to calculate the effective moment of the $L^{3+} =$ Gd, Yb, and Eu ion by removing the contribution of the Eu^{2+} using $2\mu_L^2 = \mu_{\text{eff}}^2 - 7.94^2$ (see Table I), where μ_{eff} is the effective magnetic moment extracted from the χ measurements of the EuL_2O_4. These μ_L values obtained are found to slightly deviate from the theoretically calculated ion.[16] The magnetic interactions between the L^{3+} should therefore contribute to the magnetic behavior; as a result, the triangular frustrated geometry on the LO_2 *zigzag* chain should play a role in determining their magnetic ground states.

In the μSR experiments, the powder sample was placed in a small Al-coated Mylar envelope. The sample was then placed onto a low-background sample holder in a liquid-He flow cryostat on the **M20** surface muon channel at TRIUMF, Vancouver, Canada. Zero-field (ZF) and weak-transverse-field (wTF) spectra were gathered in the T range between 1.8 and 30 K. The ZF-μSR technique is a sensitive probe of local magnetic [dis]order through the precession of the muon spin in internal magnetic fields at the muon's interstitial sites. In the wTF-μSR technique, a field is applied perpendicular to the muon-spin direction; the applied field H_{TF} is weak compared to any spontaneous internal fields in a magnetic ordered phase. Thus, the amplitude (asymmetry) of the μSR precession at the frequency of H_{TF} is a measure of the volume fraction of the sample that does *not* exhibit local magnetic order.[17]

III. RESULTS

A. L = Lu, Eu, Yb

To probe the magnetic phase of EuL_2O_4, we concentrate mainly on the μSR-spectra measured below T_N. The raw ZF data taken for $L =$ Lu, Eu, and Yb, is unlike the $L =$ Gd compound, hence is discussed subsequently. As a typical example of the spectra for $L =$ Lu, Eu, and Yb, Fig. 2(a) depicts the raw ZF data taken at $T = 1.8$ K. An oscillation due to the ordered state is observed and as an example the Fourier transform (FT) for $L =$ Lu is shown is Fig. 2(b). The spectrum clearly indicates a single frequency at ~60 MHz. The ZF-μSR spectra can be fitted with the sum of an exponentially relaxing

TABLE I. Key results of the bulk and local data obtained by SQUID and μSR. T_N and θ_{CW} are the Neél and Curie-Weiss temperatures, respectively, μ_L is the effective moment of the L ion. φ is the initial phase measured at $T = 1.8$ K with a cosine fitting function [Eq. (1)]. $F(t)$ is the fitting function as described in the text, χ^2/NDF is the reduced χ^2 goodness of fit parameter when the raw data are fitted with $F(t)$. β_{BCS} is the BCS energy gap critical exponent, the ground state is obtained from the ZF-μSR data below T_N, and β is the critical exponent measured above T_N.

	SQUID			μSR					
L	T_N (K)	θ_{CW} (K)	μ_L (μ_B)	φ (deg.)	$F(t)$	χ^2/NDF	β_{BCS}	Ground state	$\beta(T > T_N)$
Lu	5.7	9.8(7)	...	1.67(17)	$\cos(\omega_{\text{AF}}t + \varphi)$	1.3(1)	0.489(3)	Static AF	0.65(3)
Eu	5.4	−32.7(6)	3.83(1)	42(20)	$J_0(\omega_{\text{AF}}t)$	1.03(5)	0.36(2)	Mixed AF/SDW	0.58(3)
Yb	6.3	−32(2)	4.77(1)	158(6)	$J_0(\omega_{\text{AF}}t)$	1.08(7)	0.306(4)	IC-SDW	0.68(4)
Gd	5.6	−4.8(3)	7.82(2)	...	...	...	...	Dynamic AF	Not measured

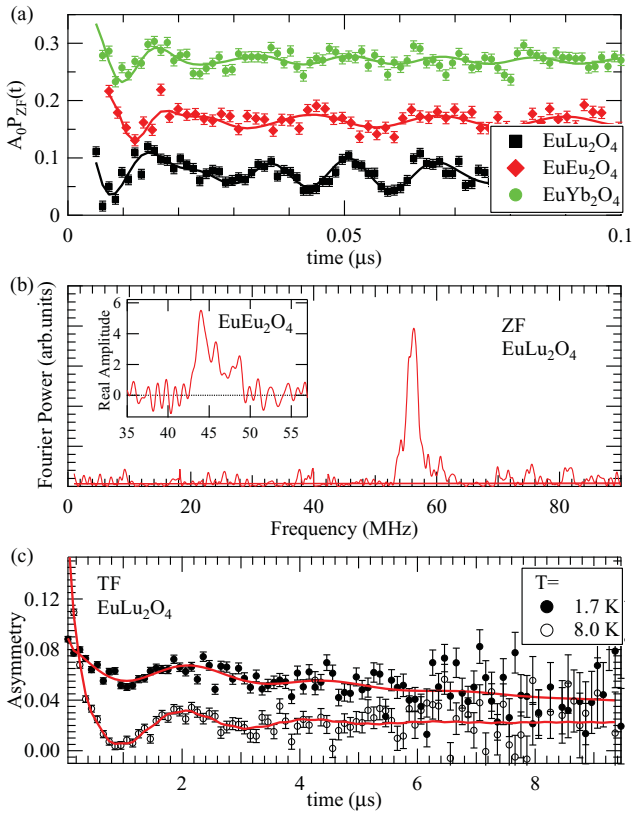

FIG. 2. (Color online) (a) The raw ZF data of EuL_2O$_4$, taken at $T = 1.8$ K, solid lines demonstrate the fit. The data of $L =$ Eu, Yb are shifted by +0.1 and +0.2 for clarity. (b) The ZF FT of EuLu$_2$O$_4$, taken at $T = 1.8$ K; inset shows the real part of the FT of EuEu$_2$O$_4$ at $T = 1.8$ K. (c) Measurements in wTF taken at 1.7 and 8.0 K; the asymmetry of the 1.7 K data is shifted by 0.05 for clarity. The solid lines indicate the fits.

cosine function, a fast relaxing component and a 1/3 tail due to the powder form of the samples,

$$A_0 P_{ZF}(t) = A_0\big[A_{slow}\big(\tfrac{2}{3}\cos(\omega_{AF}t+\varphi)\exp(-\lambda_{AF}t) + \tfrac{1}{3}\exp(-\lambda_{tail}t)\big) + A_{fast}\exp(-\lambda_{fast}t)\big], \quad (1)$$

where A_0 is the initial asymmetry, determined by measurements of a Ag plate prior to the sample measurements. The frequency $\omega_{AF} = 2\pi f$ and relaxation rate λ_{AF} arise from the ordered AF phase. The fast relaxing component is due to fluctuating moments, which give only a minor contribution, as evidenced by its small asymmetry, $A_{fast} \ll A_0$.

The oscillating signal in the spectra could also be fitted with a zeroth-order Bessel function of the first kind [$J_0(\omega_{AF}t)$] instead of a cosine [$\cos(\omega_{AF}t+\varphi)$ in Eq. (1)].[20] This has been found to be appropriate in numerous quasi-1D systems.[3,18] A ZF spectrum described by J_0 is a key signature that the muon experiences an incommensurate (IC) field distribution, and as such points to a spin-density-wave (SDW) ground state.[19] However, due to the fast damping of the oscillating signal, it is hard to justify one function over the other.[20] One of the characteristics of an IC-SDW which suggests a Bessel function fit is a nonzero phase, φ. In EuEu$_2$O$_4$ and EuYb$_2$O$_4$, the phase changes with T particularly below the vicinity of T_N with $\varphi(T = 1.8\text{K}) = 42(20)^\circ$ and $158(6)^\circ > 0$, respectively. Hence, these compounds are more likely to possess a mixed IC-AF phase, or an IC phase. The real part of the FT, which reflects the local field distribution, also shows the characteristic tail of an IC modulation in these compounds [see inset in Fig. 2(b)]. In contrast, the EuLu$_2$O$_4$ shows a negligible initial phase [$\varphi(T = 1.8\text{ K}) = 1.67(17) \approx 0^\circ$]; thus, it is more likely to assume a commensurate magnetic phase.

We can also use the wTF data as a complementary measurement. In the paramagnetic phase, the wTF-spectrum is fitted with a slow exponentially relaxing cosine function:

$$A_0 P_{TF}(t) = A_{TF}\cos(\omega t+\varphi)\exp(-\lambda_s t), \quad (2)$$

where $\omega = \gamma_\mu H_{TF}$ is the muon Larmor frequency, with $\gamma_\mu =$ 13.554 kHz/G, and $H_{TF} = 30$ Oe is the applied wTF. Below T_N, an additional term is needed to fit the signal, due to the AF ordered phase:

$$A_0 P_{TF}(t) = A_{TF}\cos(\omega t+\varphi)\exp(-\lambda_s t) + A_{AF}F(t)\exp(-\lambda_{AF}t), \quad (3)$$

where F is a cosine or a Bessel function, as in the ZF measurements. As an example, the raw wTF-spectra of $L =$ Lu obtained at 1.7 and 8.0 K are plotted in Fig. 2(c).

Figure 3 shows the T dependence of f extracted from the fits for the $L =$ Lu, Eu, and Yb samples. Obviously, the moment size is not the sole parameter which influence the internal field and therefore the muon precession frequency, for example, the magnetic order should also be taken into consideration. Nevertheless, the difference between the three compounds are apparent in the slopes of the $f(T)$ curve, for instance, the slope below $T = 4$ K is larger in $L =$ Lu than that of Eu and Yb. The common feature, however, is the behavior of $f(T)$ which is typical of SDW order. That is, the $f(T)$ curve follows the theoretical T dependence of the BCS gap energy,[21] i.e., $f = f_{T\to 0}\times\tanh[1.74\times(1-T/T_N)^{\beta_{BCS}}]$, as seen by the solid lines in Fig. 3. The parameter β_{BCS} depends on the Hamiltonian, or phase, describing the magnetic interaction in the experimental system. In EuLu$_2$O$_4$, the fit to this equation yields the expected $\beta_{BCS} = 1/2$ from mean-field theory[22] [$\beta_{BCS} = 0.489(3)$]. Whereas in EuEu$_2$O$_4$ and EuYb$_2$O$_4$, it reveals β_{BCS} to be decreasing with increasing magnetic moment [$\beta_{BCS} = 0.36(2)$ and $\beta_{BCS} = 0.302(4)$, respectively]. As an example, $\beta_{BCS} = 0.326$ is expected in the one-spin-dimensionality Ising lattice.[23] Regardless of the absolute value of β_{BCS}, the difference between the values in the different compounds implies that the large Yb moments along the *zigzag* chain affect the magnetic order and alters the ground state.

B. $L =$ Gd

In EuGd$_2$O$_4$, on the other hand, ZF and wTF measurements below T_N do not show a clear formation of static AF order. Instead a slow relaxation is observed, as seen in the inset of Fig. 4. This was also confirmed using the **HiTime** spectrometer on the **M15** channel at TRIUMF, which currently has the highest time resolution in the world. The ZF spectrum is well fitted globally by a stretched exponential relaxation function:

$$A_0 P_{ZF}(t) = A_0\exp[-(\lambda_{ZF}t)^\beta], \quad (4)$$

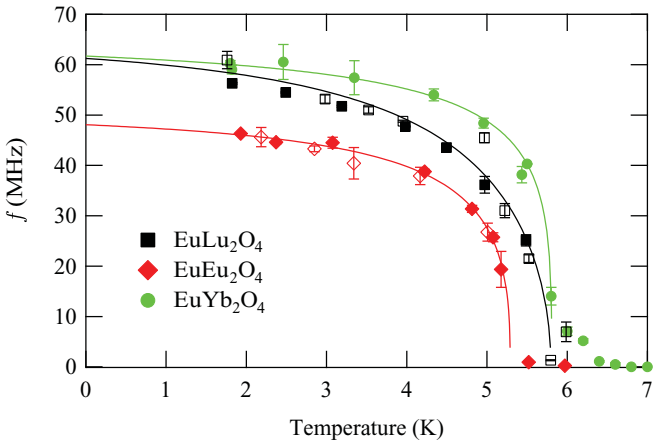

FIG. 3. (Color online) Temperature dependence of the muon-spin precession frequency ($f \equiv \omega_{AF}/2\pi$) of L = Eu, Lu, Yb. Filled symbols were measured in ZF, hollow symbols were measured in wTF. Lines indicate the T dependence of the BCS gap energy.

where $\beta = 0.42(8)$ and A_0 were common for all T. Here, $\beta = 1/2$ suggests a dilute disordered magnet,[24] whereas $\beta = 1/3$ characterizes a dense disordered phase.[25] As expected, the longitudinal relaxation ($\lambda_{ZF} = 1/T_1$) shows critical behavior as $T \to T_N$. The main panel of Fig. 4 displays the T dependence of λ_{ZF} along with the $\chi(T)$ curve of $EuGd_2O_4$. Clearly, the ZF-μSR data tracks the bulk χ measurement. Since the two measurements (local and bulk) do not indicate a Curie tail, which is expected at low T due to impurities, the absence of static AF order, detected by ZF-μSR, below T_N is most likely an intrinsic feature of $EuGd_2O_4$, and not due to impurities. Hence, we argue that the strong Gd moments destroy the local magnetic order, whereas such order is seen in the other compounds having smaller moments. This conclusion is supported by the fact that $EuYb_2O_4$, in which Yb has the second largest magnetic moments in our study, also shows a weak IC-SDW behavior. Hence, we claim that in L = Lu, the AF order is caused only due to the Eu^{2+} ions (7.94 μ_B), while in L = Eu and Yb, the moment perturb the AF order of the Eu^{2+}. In L = Gd, the moment is comparable to the Eu, resulting in a small internal field at the muon site. Note that

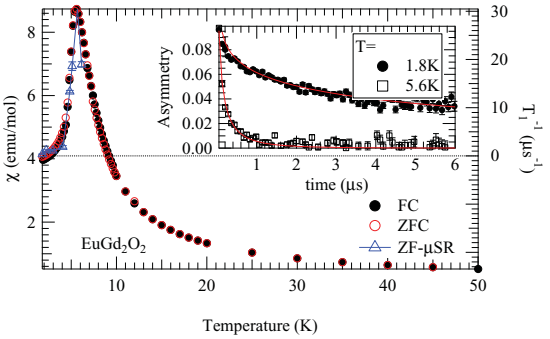

FIG. 4. (Color online) (Inset) The raw ZF asymmetries of $EuGd_2O_4$ taken at T = 1.8 and 5.6 K; lines denote the fits. (Main panel) Temperature dependence of the zero-field (ZFC) and field-cooled (FC) susceptibilities (left axis) and the muon longitudinal relaxation rate, T_1^{-1} (right axis). The line is a guide to the eye.

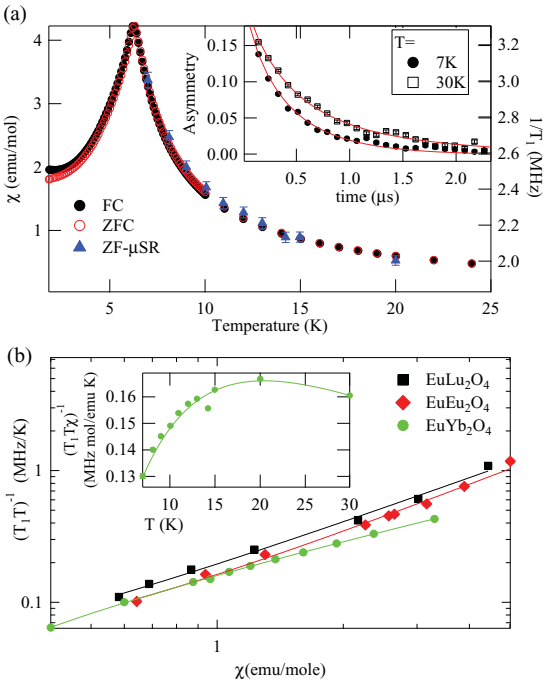

FIG. 5. (Color online) $EuYb_2O_4$: (a) inset shows the raw ZF asymmetries taken at 7 and 30 K. Main panel depicts the $EuYb_2O_4$ temperature dependence of the zero-field (ZFC) and field-cooled (FC) susceptibility $\chi = M/H$ (left axis) and the muon T_1^{-1} relaxation rate (right axis). (b) Inset shows the temperature dependence of $1/(T_1T\chi)$. Main panel displays $(T_1T)^{-1}$ versus χ for $EuLu_2O_4$, $EuEu_2O_4$, and $EuYb_2O_4$. The solid lines in the figures display the fit.

unlike the Lu, Eu, and Yb ions, which include a crystal electric field (CEF) interaction, the Gd ion does not posses CEF.

C. T_1 measurements of EuL_2O_4

In order to differentiate between the EuL_2O_4 with L = Lu, Eu, and Yb, we turn to the longitudinal relaxation rate, T_1, extracted from the ZF data fittings. Consequently, ZF-μSR was also measured above T_N, up to 30 K. These are compared with respect to their χ. The T dependence of χ in $EuYb_2O_4$ is plotted in Fig. 5(a). A clear transition is seen at $T_N = 6.3$ K, indicating the AF phase below T_N. The data in the paramagnetic phase were fitted globally to a phenomenological stretched exponential [as in Eq. (4)], with a fast relaxing component, as in the ordered state. The initial asymmetry A_0 and $\beta = 0.68(4)$ were common in all data sets. On the right axis of Fig. 5(a), we plot the ZF-μSR longitudinal relaxation rates, T_1^{-1}, extracted from the fits. The T_1^{-1} data clearly fits the $\chi(T)$ data, showing the enhancement and slowing down of the fluctuations as $T \to T_N$. Such measurements were also performed on the paramagnetic phases of $EuLu_2O_4$ and $EuEu_2O_4$. Spin-fluctuation theories suggest that $(T_1T)^{-1} \propto \chi^n$.[26] Thus, the main panel of Fig. 5(b) shows plots of $(T_1T)^{-1}$ versus χ for these compounds. Fits to this function, indicated by the solid lines, reveal n = 1.15(5), 1.25(6), and 0.72(2), for L = Lu, Eu, and Yb, respectively. The negative curvature of $EuYb_2O_4$ suggests a slightly different scenario, where the relaxation is driven by random field fluctuations,[27] hence $(T_1T\chi)^{-1} = A\tau/(1+\omega^2\tau^2)$, where $\tau \propto T^{-n}$ is the

correlation time and ω is the Larmor frequency at the muon site. We find $\tau = T^{-0.684(2)}$. This fit is represented in the inset of Fig. 5(b).

To summarize, here we were able to show that with the synthesis of different *zigzag* magnetic moments, we can tune the system into a specific ground state phase. μSR and susceptibility measurements were performed on four EuL_2O_4 compounds (where L is the lanthanide, Eu, Gd, Yb, and Lu). The bulk χ data reveal that an AF transition takes place in all at $5.4 \leqslant T \leqslant 6.3$ K; On a local scale, μSR indicates the formation of a static AF (in $L =$ Lu), a mixed AF/IC-SDW ($L =$ Eu), and an IC-SDW ($L =$ Yb) ordered phase. In $EuGd_2O_4$, a dynamic disordered phase is suggested. Thus, the difference in the magnetic moment, arising from the lanthanide ion (L^{3+}), in these quasi-1D *zigzag* chains reveals that static AF order becomes dynamic as the magnetic moment along the *zigzag* chain increases.

ACKNOWLEDGMENTS

We are grateful to the staff of TRIUMF for assistance with the μSR experiments. J.H.B. is supported at UBC by NSERC of Canada and (through TRIUMF) by NRC of Canada. K.H.C. is supported by NSERC of Canada and (through TRIUMF) by NRC of Canada.

*oren@triumf.ca

†Present address: Research Center for Neutron Science and Technology, Comprehensive Research Organization for Science and Society, Tokai, Ibaraki 319-1106, Japan, and J-PARC Center, JAEA, Tokai, Ibaraki 319-1195, Japan.

[1] Z. Q. Mao, T. He, M. M. Rosario, K. D. Nelson, D. Okuno, B. Ueland, I. G. Deac, P. Schiffer, Y. Liu, and R. J. Cava, Phys. Rev. Lett. **90**, 186601 (2003).

[2] S. Kimura, T. Takeuchi, K. Okunishi, M. Hagiwara, Z. He, K. Kindo, T. Taniyama, and M. Itoh, Phys. Rev. Lett. **100**, 057202 (2008).

[3] O. Ofer, Y. Ikedo, T. Goko, M. Mansson, J. Sugiyama, E. J. Ansaldo, J. H. Brewer, K. H. Chow, and H. Sakurai, Phys. Rev. B **82**, 094410 (2010).

[4] T. Yamauchi, Y. Ueda, and N. Mori, Phys. Rev. Lett. **89**, 057002 (2002).

[5] T. Yamauchi and Y. Ueda, Phys. Rev. B **77**, 104529 (2008).

[6] A. A. Zvyagin and S.-L. Drechsler, Phys. Rev. B **78**, 014429 (2008).

[7] A. A. Zvyagin, Phys. Rev. B **81**, 224407 (2010).

[8] S. Furukawa, M. Sato, and A. Furusaki, Phys. Rev. B **81**, 094430 (2010).

[9] T. Hikihara, L. Kecke, T. Momoi, and A. Furusaki, Phys. Rev. B **78**, 144404 (2008).

[10] T. Hikihara, T. Momoi, A. Furusaki, and H. Kawamura, Phys. Rev. B **81**, 224433 (2010).

[11] K. Hirose, Y. Doi, and Y. Hinatsu, J. Solid State Chem. **182**, 1624 (2009).

[12] A. Niazi, S. L. Budko, D. L. Schlagel, J. Q. Yan, T. A. Lograsso, A. Kreyssig, S. Das, S. Nandi, A. I. Goldman, A. Honecker, R. W. McCallum, M. Reehuis, O. Pieper, B. Lake, and D. C. Johnston, Phys. Rev. B **79**, 104432 (2009).

[13] K. Yamaura, M. Arai, A. Sato, A. B. Karki, D. P. Young, R. Movshovich, S. Okamoto, D. Mandrus, and E. Takayama-Muromachi, Phys. Rev. Lett. **99**, 196601 (2007).

[14] H. Karunadasa, Q. Huang, B. G. Ueland, J. W. Lynn, P. Schiffer, K. A. Regan, and R. J. Cava, Phys. Rev. B **71**, 144414 (2005).

[15] Y. Doi, W. Nakamori, and Y. Hinatsu, J. Phys. Condens. Matter **18**, 333 (2006).

[16] C. Kittel, *Introduction to Solid State Physics*, 7th ed. (John Wiley & Sons, Inc., New Jersey, 1995).

[17] G. M. Kalvius, D. R. Noakes, and O. Hartmann, in *Handbook on the Physics and Chemistry of Rare Earths*, edited by K. A. Gschneidner Jr., L. Eyring, and G. H. Lander (North-Holland, Amsterdam, 2001), Vol. 32, Chap. 206; J. H. Brewer, *Encyclopedia of Applied Physics* (VCH Publishers, New York, 1994) Vol. 11, pp. 23–53.

[18] J. Sugiyama, Y. Ikedo, K. Mukai, J. H. Brewer, E. J. Ansaldo, G. D. Morris, K. H. Chow, H. Yoshida, and Z. Hiroi, Phys. Rev. B **73**, 224437 (2006); J. Sugiyama, K. Mukai, Y. Ikedo, P. L. Russo, H. Nozaki, D. Andreica, A. Amato, K. Ariyoshi, and T. Ohzuku, *ibid.* **78**, 144412 (2008).

[19] J. Major, J. Mundy, M. Schmolz, A. Seeger, K.-P. Doring, K. Furderer, M. Gladisch, D. Herlach and G. Majer, Hyperfine Interact. **31**, 259 (1986); A. Amato, R. Feyerherm, F. N. Gygax, A. Schenck, H. v. Lohneysen, and H. G. Schlager, Phys. Rev. B **52**, 54 (1995); N. Papinutto, M. J. Graf, P. Carretta, A. Rigamonti and M. Giovannini, Physica B **359**, 89 (2005).

[20] In $EuLu_2O_4$, the T-averaged reduced-χ^2 value achieved from the fit to Eq. (1) was 1.30(18) and 1.31(15) from the fit with J_0; in $EuEu_2O_4$, the reduced-χ^2 were 1.16(13) and 1.03(5), with Eq. (1) and J_0; in $EuYb_2O_4$, 1.05(8) With Eq. (1); 1.08(7) with J_0.

[21] G. Grüner, *Density Waves in Solids* (Addison-Wesley-Longmans, Reading, 1994) Chap. 4, and references cited therein.

[22] M. Tinkham, *Introduction to Superconductivity* (McGraw-Hill Inc., New York, 1996).

[23] Theoretical values for β_{BCS} can be found in table 5.1 of M. F. Collins, *Magnetic Critical Scattering* (Oxford University Press, Oxford, 1989).

[24] Y. J. Uemura, T. Yamazaki, R. S. Hayano, R. Nakai, and C. Y. Huang, Phys. Rev. Lett. **45**, 583 (1980).

[25] A. T. Ogielski, Phys. Rev. B **32**, 7384 (1985).

[26] T. Moriya, *Spin Fluctuations in Itinerant Electron Magnetism* (Springer-Verlag, Berlin 1985).

[27] P. Carreta, *NMR-MRI, μSR and Mössbauer Spectroscopies in Molecular Magnets*, edited by P. Carretta and A. Lascialfari (Springer, Milan, 2007).